Effects of Cold Deformation Prior to Sensitization on Intergranular Stress Corrosion Cracking of Stainless Steel

R. Singh,[‡,*] J. Swaminathan,* S.K. Das,* B. Ravi Kumar,* and I. Chattoraj*

ABSTRACT

The effects of deformation, prior to sensitization, on intergranular stress corrosion cracking (IGSCC) were studied on the AISI 304 (UNS S30400) stainless steel (SS). The degree of sensitization (DOS) was quantified by the double loop electrochemical potentiokinetic reactivation (DL-EPR) method. The susceptibility to IGSCC was investigated by the slow strain rate test (SSRT) carried out in polythionic acid (PTA) solutions. The results were complemented by scanning electron microscopy (SEM) fractographs. Deformation was found to accelerate sensitization, and a peak in sensitization vs. deformation was always observed. This peak was found to shift toward lower deformations with an increase in sensitization temperature. At 700°C, prior deformation is able to desensitize or heal the SS after 24 h. IGSCC was observed in AISI 304 SS after some treatments. No one-to-one correspondence was observed between IGSCC and DOS; this could be explained by the fact that the DOS measured by the DL-EPR indicates the depleted regions below ~15% Cr, whereas IGSCC depends on the availability of continuous grain boundary paths that are chromium-depleted, along with strain rate and environment (pH, temperature, etc.). Deformation prior to sensitization causes carbide formation and chromium depletion to occur near dislocations within the grain interiors, in addition to along grain boundaries. The DOS does not differentiate between these interior regions and the grain boundary regions, and shows a total value accounted for chromium depletion. However, IGSCC occurs only when there is chromium depletion along grain boundaries and therefore these intragrain regions further reduce the correlation between the DOS and IGSCC susceptibility. Deformation close to or beyond 60% was found to prevent IGSCC of AISI 304 SS, irrespective of the sensitization temperature or DOS value.

KEY WORDS: deformation, double loop electrochemical potentiokinetic reactivation, intergranular stress corrosion cracking, polythionic acid, sensitization, slow strain rate test

INTRODUCTION

Sensitization is a common phenomenon in stainless steels (SS) when they are exposed to temperatures ranging from about 400°C to 800°C.[1-20] Classical sensitization results from the nucleation and growth of chromium carbide along grain boundaries (in solution-annealed SS and nickel alloys) with simultaneous depletion of chromium in adjacent grain boundary regions. The extent of chromium depletion in near grain boundary regions is limited by the equilibrium concentration of chromium at the carbide-matrix interface. The equilibrium chromium level depends on the temperature, the chromium activity coefficient, the carbon activity, and the equilibrium constant for carbide formation. Hall and Briant showed the equilibrium chromium concentrations to be 6.6, 8.4, and 10.8 wt% in AISI 316LN[(1)] (UNS S31603)[(2)] sensitized at 600, 650, and 700°C, respectively.[21] Sensitization occurs in the temperature range where carbide is thermodynamically stable (<900°C) and chromium has sufficient diffusivity (>500°C); both the kinet-

Submitted for publication June 2004; in revised form, January 2005.

‡ Corresponding author. E-mail: raghujog@yahoo.com.in.
* National Metallurgical Laboratory, ACC Division, Jamshedpur, 831007, India.

(1) American Iron and Steel Institute (AISI), 1140 Connecticut Ave., St. 705, Washington, DC 20036.
(2) UNS numbers are listed in *Metals and Alloys in the Unified Numbering System*, published by the Society of Automotive Engineers (SAE International) and cosponsored by ASTM International.

0010-9312/05/000185/$5.00+$0.50/0

ics of chromium diffusion and carbide nucleation are enhanced by introducing deformation.[4-5,15] While correlations were developed by several researchers between the chromium concentration (in equilibrium with chromium carbide) and bulk carbon content, the diffusivity of carbon was assumed to be much higher than the chromium, and the carbon content adjacent to carbide particles was considered to be the same as in the matrix (bulk).[4-5,15] Diffusion of chromium is the rate-limiting process in nucleation and growth of chromium carbide. The susceptibility of sensitized SS to intergranular corrosion results when chromium at the carbide-matrix interface decreases below a critical level required to maintain passivity. Bruemmer, et al.,[22] measured the concentration of chromium in the depleted region (Type 304 [UNS S30400] and Type 316 [UNS S31600] SS) using scanning transmission microscopy with energy-dispersive x-ray spectroscopy (STEM-EDS) and showed that the regions containing chromium below ~12.5 wt% to 13.5 wt% were attacked in the electrochemical potentiokinetic reactivation (EPR) test.

In deformed SS, carbide nucleation can occur at substantially lower temperatures than in undeformed SS.[15-17,22] After nucleation, growth can occur (in undeformed and deformed SS) at <<400°C, typically known as low-temperature sensitization (LTS).[17] In welded or slow-cooled (during solution annealing) SS, when exposed to service environments such as nuclear power plants where the operating temperature is ~300°C, severe chromium depletion may occur during the growth of carbide particles.

It is well established that stress corrosion cracking (SCC) is accelerated by chromium-depleted grain boundaries. Sensitization and, therefore, intergranular stress corrosion cracking (IGSCC) is known to depend upon the times and temperatures of exposure. Sensitization has been shown to be affected by the variables like prior deformation, deformation-induced martensite, grain size, and grain boundary orientation.[18-34] Solomon[18] showed that the prior deformation of AISI 304 SS containing different amounts of carbon contents increased the cooling rate for sensitization by a factor >7, compared to the cooling rate measured for an annealed specimen. In another study on the effect of strain generated during cooling (simulated to weld-induced sensitization) on sensitization, they showed that strain as low as 5% (if single heating and cooling cycle is used) and ~0.8% per cycle (if multiple heating and cooling cycles are used) could enhance the sensitization.[20] Briant and coworkers[21,24] showed that prior deformation alone (without introducing martensite, such as in AISI 316 SS) increases the kinetic of sensitization only at temperatures where undeformed SS readily sensitized. However, AISI 304 SS, which contained deformation-induced martensite, experienced rapid sensitization at <600°C and produced rapid healing. AISI 304 SS suffered from the transgranular corrosion, whereas AISI 316 SS (without martensite) predominantly experienced intergranular corrosion.[21,24] Advani and coworkers[26-28] found transgranular chromium depletion and transgranular corrosion along the sites created by the prior straining of SS. Beltran, et al.,[29] reported that the increase in strain and the decrease in grain size accelerated the sensitization-desensitization process in AISI 304 SS, sensitized at 625°C and 775°C. Recently, it has been reported that prior deformation <10% increased intergranular corrosion, whereas >30% caused an increase in transgranular corrosion.[30] Parvathavarthini and Dayal[34] showed that deformation <15% greatly accelerates sensitization kinetics, whereas beyond 15% it desensitizes the AISI 316 SS.[34]

The effects of the combination of sensitization and prior deformation (which may be encountered during welding, thermo-mechanical processing, etc.) on the corrosion failures are especially important to understand in situations where components are exposed to the corrosive environment under stresses (residual or service). The behavior of SS experiencing simultaneous prestraining and sensitization is important to investigate, especially when sensitization and cold deformation, in isolation, are known to change SCC behavior to varying extents.[18-38] Results on the effect of cold working alone differ. Kowaka and Fujikawa[36] showed an increase in SCC susceptibility of AISI 304 SS up to 20% deformation in boiling magnesium chloride ($MgCl_2$) solution. Muraleedharan, et al.,[38] showed an insignificant effect of cold work on AISI 304 SS (in boiling $MgCl_2$ solution at 154°C) when tests were carried out at a constant stress (112 MPa); however, SCC resistance deteriorated when similar experiments were performed at a stress level of 40% of the yield stress (94.8 MPa to 364.8 MPa for 0 to 56% deformed AISI 304 SS). Extensive research has been carried out on the SCC behavior of sensitized SS to understand the effects of various environmental species as well as their concentration on IGSCC. This includes studies in polythionic acid (PTA) solutions,[39-41] thiosulfate ($M_2S_2O_3$),[42-44] oxygenated high-purity water,[45] boiling magnesium chloride/sodium chloride ($MgCl_2$/NaCl) solutions.[30,46-48] The focus of some of these studies was to look at the propensity of IGSCC with varying time, temperature, potential, and their associated effect on grain boundary chromium depletion.[49] However, a few have attempted to correlate sensitization with IGSCC[45,48-54] and have inferred that either no relationship exists[50] or it exists in some way.[45,48-49,51-54] One of the origins of this conflict is that there was no method available to quantify the sensitization, which is now available as an EPR method that can quantify the sensitization in terms of the degree of sensitization (DOS). This provides a better quantitative as well as qualitative correlation between sensitization and IGSCC of SS. The results for Alloy 600 (UNS N06600), using the EPR method, indicated that no correlation exists between DOS and IGSCC susceptibility in sodium tetrathionate ($Na_2S_4O_6 \cdot 2H_2O$) solutions;[50-51] however, the depth of the chromium depletion was found to correlate with IGSCC. IGSCC susceptibility of SS in various environments was found to correlate with the minimum chromium level in the depletion regions along grain boundaries.[52-55] Others did observe a good correlation between EPR-DOS of SS sensitized at constant temperature for varying times with IGSCC, but they observed a poor correlation when specimens were sensitized at different temperatures at constant time.[48] Nonunanimous findings on the relationship between DOS and IGSCC could be due the fact that which parameter (such as chromium-depleted width, minimum chromium level, or both) of the chromium-depleted region that the DOS follows is not clear.[22,52-53,56-57]

It is of great industrial relevance to establish such correlations since EPR-DOS is a fast, nondestructive method for measuring sensitization, unlike other test methods.[58] Such investigations may provide good inputs to modify the DOS measuring technique to improve its ability to reflect IGSCC susceptibility. The sensitization of prior cold-deformed SS is of relevance to thermo-mechanical processing, which is more complex than the sensitization of simple solution-annealed materials.[18-34] Therefore, the DOS of such a complexed material's state is more difficult to correlate to IGSCC.[18-34,59] Recent efforts in this direction have attempted such an objective utilizing the U-bend test in boiling $MgCl_2$ solution,[31] where steels were sensitized at 670°C for short durations (up to 1 h); although making U-bend specimens from plates of different thicknesses may be ambiguous because other variables are affected.

Investigations were undertaken to evaluate the effects of deformation on the DOS of AISI 304 SS and correlate it with IGSCC susceptibility. This was accomplished by deforming SS (with an initial thickness of ~3.2 mm) by cold rolling to thickness reduction in the range from 0 to 80% (3.2 mm to 0.7 mm final thickness) followed by sensitization at 500, 600, or 700°C for 5 h or 24 h. The DOS was determined by the DL-EPR method and IGSCC susceptibility by using slow strain rate tests (SSRT) in polythionic acid solution, which is known to induce cracking in sensitized materials.

EXPERIMENTAL PROCEDURES

AISI 304 SS containing 0.044% C, 0.016% S, 0.039% P, 1.03% Mn, 0.7% Si, 9.9% Ni, and 18.1% Cr was used. SS sheets were cut into 150- by 80- by 32-mm pieces for cold rolling to 0 to 80% reduction in thickness. Cold rolling was performed unidirectionally at ambient temperature. In each pass, a 10% reduction in thickness was attained. Coupons were cut to study sensitization (20 mm by 20 mm) and IGSCC (80 mm by 20 mm) in SSRT. The notched tensile specimens for SSRT were fabricated using a 25-mm gauge length and 10-mm width.

Material hardness was determined using a Vickers hardness tester. Residual stresses and texture evaluation were made using a x-ray diffractometer attached with a texture goniometer. The texture measurement on the rolled surface was determined using the Schultz reflection technique[60] using specimens that were electropolished in a solution of 125 mL sulfuric acid (H_2SO_4) + 650 mL orthophosphoric acid (H_3PO_4) in 225 mL distilled water and performed at 85 ± 2°C under controlled current (~1.5 A) and potential (~8.0 V) conditions with a copper rod used as a cathode.[33]

The DOS was determined by the double loop electrochemical potentiokinetic reactivation (DL-EPR) method at ambient temperature. Samples were polished using up to 1,200 grit emery paper followed by cloth polishing with diamond paste (~0.03 micron) and degreasing in acetone (CH_3COCH_3) solutions. The test solution (0.5 M H_2SO_4 + 0.01 M potassium thiocyanate [KSCN]) was prepared from reagent-grade chemicals in distilled water. Before polarizing, the samples were cathodically cleaned at a potential of –900 mV with respect to a saturated calomel electrode (SCE) for 120 s. Scanning was initiated at a potential of –100 mV (with respect to the open-circuit potential [OCP]) and reversed at a potential of 300 mV_{SCE} at a scan rate of 6 V/h. A SCE was used as a reference electrode. The DOS was evaluated by measuring the ratio of I_r/I_a, where I_r was the peak reactivation current density and I_a was the peak activation current density.

IGSCC studies were carried out by conducting SSRT in polythionic acid solutions at OCP in ambient conditions. The specimens were pulled at a constant strain rate of 5×10^{-6}/s. Polythionic acid solution was prepared by bubbling hydrogen sulfide (H_2S) gas through the sulfurous acid (H_2SO_3). The latter was produced by bubbling the sulfur dioxide (SO_2) gas in distilled water, in accordance with the ASTM specification.[61]

RESULTS AND DISCUSSION

The hardness and residual stress after deformation were measured (Table 1). The hardness of the SS after deformation was found to increase, which is caused by increasing dislocation density. The residual stresses did not show a uniform trend with increased deformation. The x-ray diffraction (XRD) measurements did not reveal the presence of deformation-induced martensite. Deformation-induced martensite in this material is expected after cold rolling; however, its absence has been reported frequently for SS processed at room temperature.[5,62-63] The (111) pole figures were obtained from the homogenized and various rolled specimens using standard projection. The pole

TABLE 1
Variation in Hardness and Residual Stress with %Deformation

%Deformation	Hardness (HV)	Residual Stress (MPa)
0	148	—
20	275	111
40	330	230
60	385	164
80	415	162

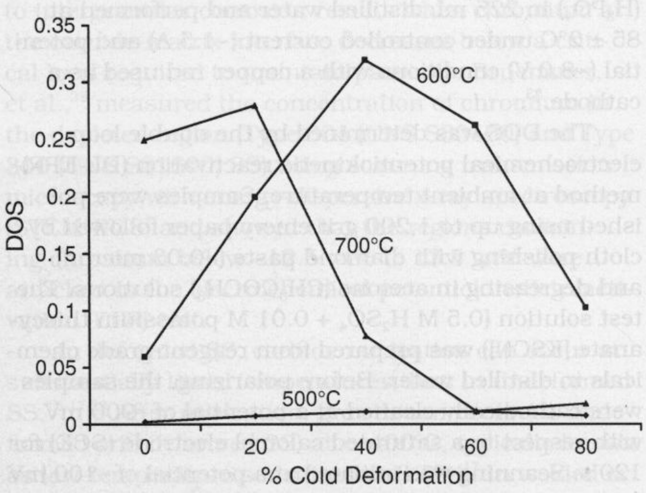

FIGURE 1. *Variation of DOS with cold deformation prior to sensitization for 5 h.*

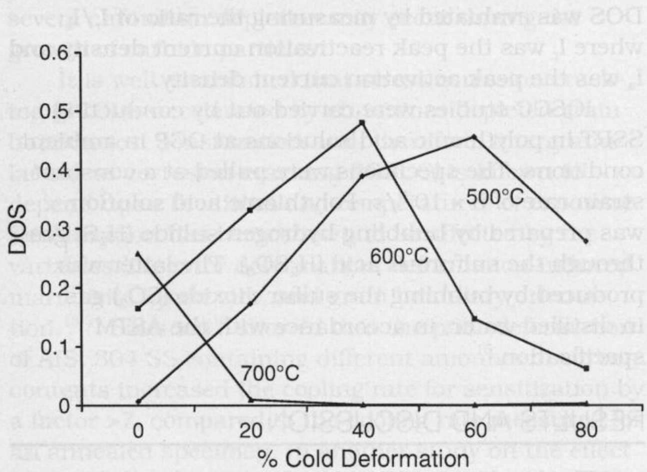

FIGURE 2. *Variation of DOS with cold deformation prior to sensitization for 24 h.*

figures showed that at 20% and 40% deformations, {110}<112> and {011}<100> were the major texture components, and their intensity was increased by further deformation. At 60% and 80% deformation, the {110}<112> component became prominent.

Sensitization

A DOS value higher than 0.05 generally corresponds to what is classically termed a "ditch structure," which describes the grain boundary appearance after an oxalic acid etch test.[58] Under such conditions the material is considered unsuitable for applications where sensitization is a concern. For the undeformed specimens, this was observed in all sensitization conditions (time/temperature combinations) except at 500°C. Introducing cold work prior to sensitization changed the sensitization kinetics as shown in Figures 1 and 2. Both figures showed that the sensitization of solution-annealed specimens increased with sensitization time and temperature, as expected. However, the cold work did affect the sensitization, except at 700°C/24 h, such that it reached a maximum in terms of DOS. Samples annealed at 500°C and 600°C (for both 5 h and 24 h) showed maximum DOS at 60% and 40% deformation, respectively. However, the DOS values for samples sensitized at 500°C/5 h were too low to show visible IG corrosion of SS. At 500°C, the DOS value for an undeformed specimen was increased by three times as the sensitization time was increased from 5 h to 24 h; however, this difference was as high as 41 times (for 60% deformation) after introducing deformation prior to sensitization. At 700°C/24 h, the maximum DOS was found for undeformed coupons, and DOS decreased to a very low value after introducing deformation. This has been termed "desensitization" or healing.

Representative post-EPR microstructures of a few sensitized specimens are given in Figures 3 and 4. Nondeformed SS shows that corrosion attack (dark regions) concentrated only along the grain boundaries and did not show attack inside the grains. The lower DOS values for samples aged at 500°C vs. those sensitized at 600°C and 700°C (Figure 1) are corroborated by the post-EPR microstructures. The maximum in the DOS value can be estimated from the post-EPR microstructures (Figures 3 and 4). It is clear from the figures that with the increase in cold deformation, corrosion attack is no longer restricted to the grain boundaries. For severe deformation (above 40%), the grain interiors are equally or more attacked than the grain boundaries. The corrosion inside the grains is from the increasing number of dislocations, vacancies, and slip bands along which carbides and chromium depletion occur, and these are also sites for corrosion during the EPR test.[19,33]

Intergranular Stress Corrosion Cracking

IGSCC tests were performed on samples, which were sensitized at 500, 600, and 700°C for 24 h. The normalized elongation and percentage reduction of area (%RA) after fracture in SSRT were calculated (Tables 2 through 4). The %normalized elongation and %normalized RA were calculated as:

$$\%\text{Normalized Elongation} = \frac{\text{Elongation in Air} - \text{Elongation in PTA}}{\text{Elongation in Air}} \times 100 \quad (1)$$

$$\%\text{Normalized RA} = \frac{\text{RA in Air} - \text{RA in PTA}}{\text{RA in Air}} \times 100 \quad (2)$$

Representative stress-elongation curves for a set sensitized at 600°C/24 h are illustrated in Figure 5. The specimens that were susceptible to IGSCC were found to fail at stresses much lower than their respective yield strengths in air. The stress-elongation behavior illustrates that the cold reduction prior to sensitization has significantly reduced the elongation in air as well as in PTA solutions (Figure 5). The ultimate tensile strength (UTS), however, was found to increase with the increase in %deformation, as expected,[64] and was accompanied by a decrease in %RA for tests in air. The mode of failure was identified using scanning electron microscopy (SEM) and is shown in Figures 6 and 7. These figures show the fractographic features of specimens sensitized at 500°C/24 h and 600°C/24 h, respectively, and show that IGSCC occurs only for specific treatment conditions. Primary and secondary IGSCC can be clearly seen (and no transgranular cracking) in Figures 6 and 7. The specimen treated at 500°C/24 h after 20% deformation failed in a completely intergranular fashion; however, a specimen deformed by 40% showed a combination of intergranular as well as ductile (dimple fracture) cracking (Figure 6). The specimens that were deformed by 0 to 40% followed by treatment at 600°C/24 h showed brittle cracking, while those that were deformed prior to sensitization at 700°C/24 h showed no sign of brittleness (Tables 2 through 4 and Figures 6 and 7) and failed in a ductile manner.

In attempting to correlate the DOS and IGSCC behavior of the nondeformed SS, it was observed that greater values of DOS and wider chromium-depleted zones (CDZ) occurred in samples treated at 700°C/24 h vs. 600°C/24 h and 500°C/24 h, whereas the 600°C/24 h specimens suffered the most severe IGSCC. This is evidence that the susceptibility to IGSCC is not fully characterized by sensitization susceptibility as measured by the DL-EPR. To explain this apparent nonconformity, the sensitivity of IGSCC and sensitization (as measured by the DL-EPR) to chromium depletion needs to be understood along with the effect of deformation. A study performed on sensitized, nondeformed AISI 304 SS in air-saturated water at 288°C concluded that the minimum chromium level, the width of CDZ, and intercarbide spacing have significant bearing on IGSCC resistance.[49] However, a critical chromium depletion width is not required, since a very narrow CDZ can also promote IGSCC. A sharp decrease in IGSCC susceptibility was observed when the chromium concentration exceeds 12% in the CDZ, although this depended on the strain rate and water chemistry. It was also noticed that the IGSCC occurred in situations (such as aged at 600°C/25 h + 900°C/25 h) where negligible DOS values were determined during the EPR tests. Bruemmer and coworkers[15-16,45] showed that EPR was controlled by the width of the region that had <15% Cr, whereas IGSCC could occur within <1% Cr depletion (depending on strain rate and water chemistry).

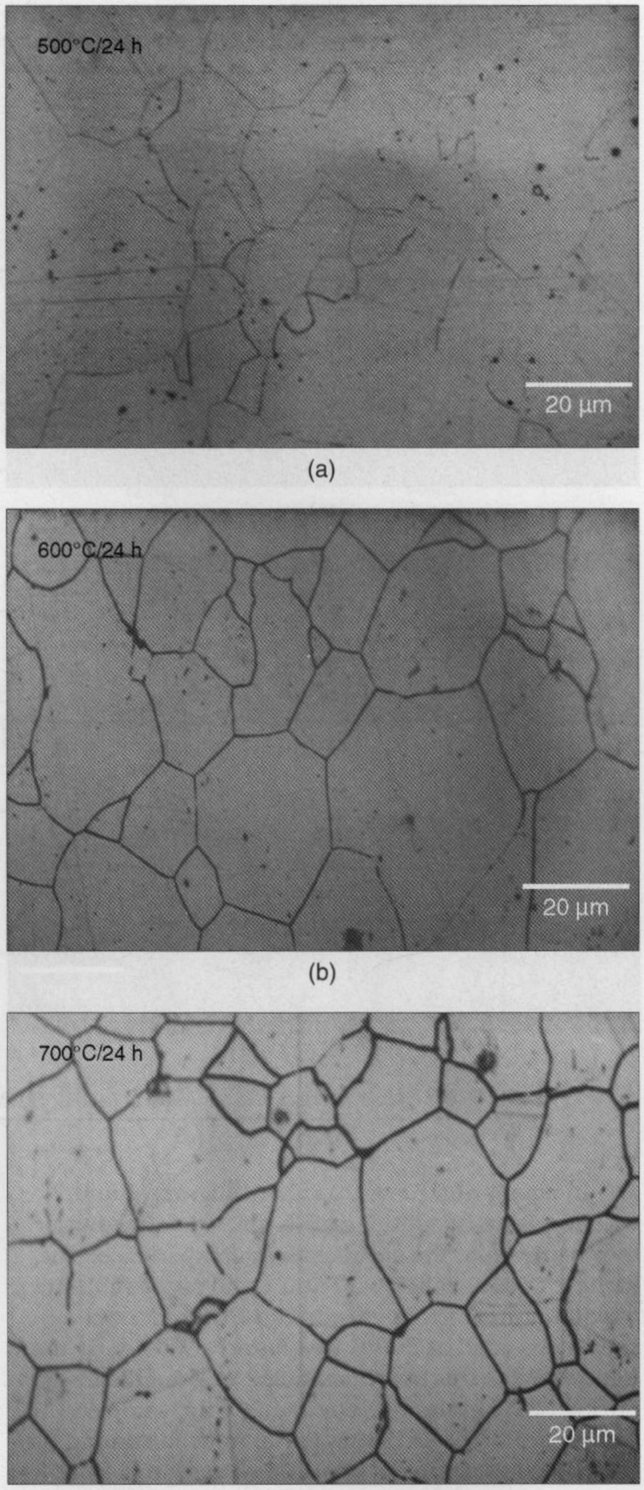

FIGURE 3. *Post-EPR microstructures of nondeformed sensitized Type 304 SS (at [a] 500°C, [b] 600°C, and [c] 700°C for 24 h).*

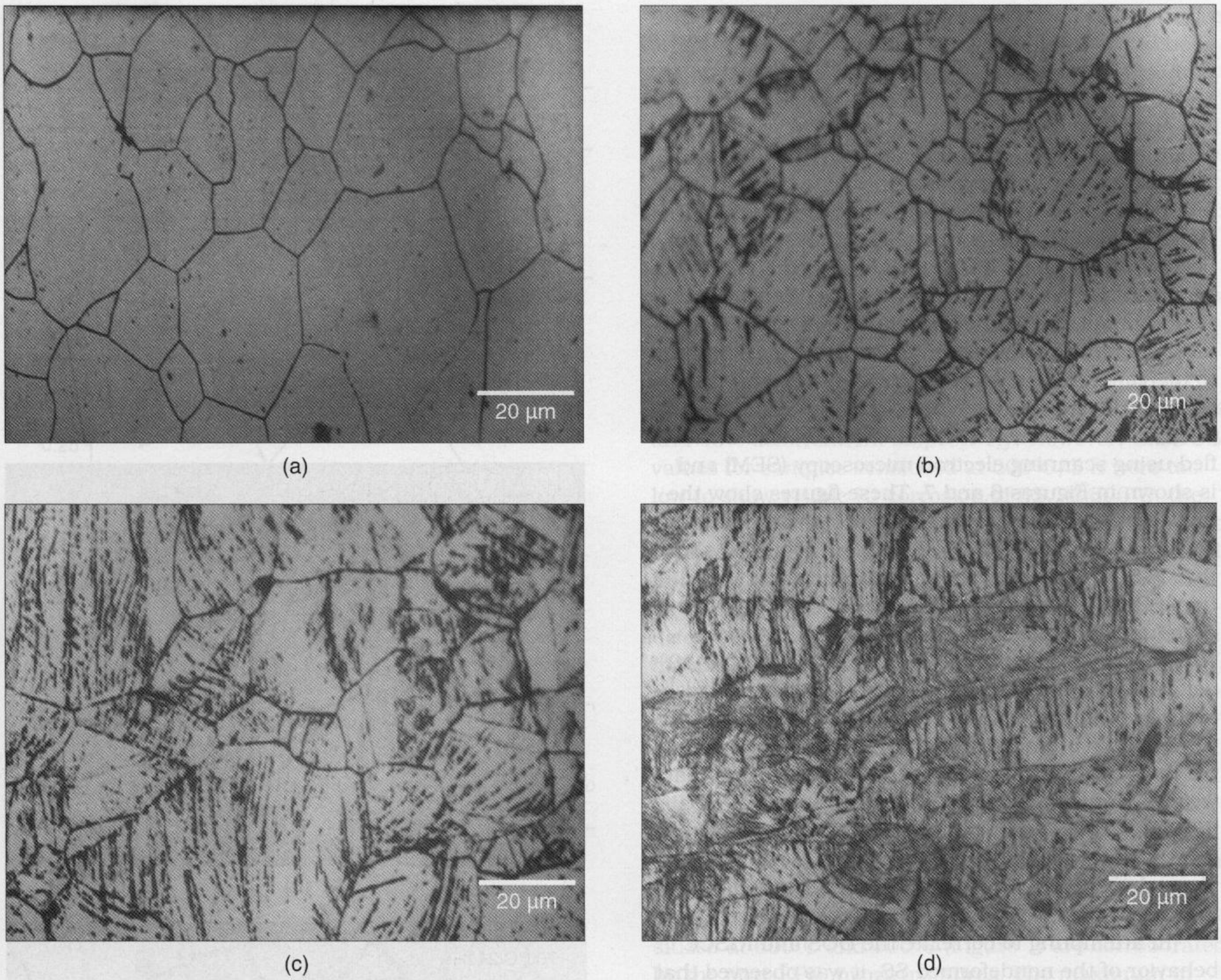

FIGURE 4. *Microstructure of SS deformed at (a) 0%, (b) 20%, (c) 40%, and (d) 60% prior to sensitization at 600°C/24 h.*

In comparing the DOS values (Figures 1 and 2) with IGSCC susceptibility of samples deformed prior to sensitization, the specimens that experienced the highest DOS at 500°C and 600°C did not exhibit the maximum IGSCC. The maximum DOS among the specimens aged at 500°C was found at 60% deformation, whereas this specimen failed in a ductile fashion during SSRT in the PTA solution. Of the samples treated at 600°C, DOS was found to be maximum for the 40% predeformed samples. However, this treatment resulted in brittle cracking in polythionic acid solutions, but the cracking severity was much less in terms of %normalized elongation and %normalized RA values compared to the sample that were predeformed by 0 to 20% (Table 3, Figure 5). At 700°C, prior deformation promotes desensitization as shown by the extremely low DOS. All these observations suggest that there may not be a direct one-to-one correspondence between the DOS determined by DL-EPR and IGSCC of prior deformed samples. This is further supported by the fact that the IGSCC varies with strain rates and environment (pH, temperature, etc.).[27] The DOS remains a reliable parameter for IGC, although it might reasonably be expected that some environments exist that produce IGC at 16% Cr vs. the ~15% Cr threshold that exists for DL-EPR.

A qualitative difference in the grain boundary attack of sensitized, nondeformed steel following EPR testing is clearly seen from the post-EPR microstructures at different temperatures (Figure 3). The attack appears wider for steel sensitized at 700°C than at 600°C or 500°C. This is because of the kinetically faster depletion of chromium at 700°C, leading to wider and more gradual chromium depletion profiles as compared to those at 600°C or 500°C. The same reasoning explains the higher EPR-DOS values obtained for undeformed samples treated at 700°C vs. lower temperatures. The essential difference in DOS and IGSCC susceptibility is a result of the difference in the governing parameters for each with regard to

TABLE 2
Percentage Elongation and Reduction of Area after SSRT of Samples Treated at 500°C/24 h

%Deformation	%Elongation (Normalized)	%RA (Normalized)	Mode of Failure
0	120	85.2	Ductile
20	47.55	56.4	Brittle
40	42.96	13.55	Brittle
60	53.35	74	Ductile
80	93.22	75.96	Ductile

TABLE 3
Percentage Elongation and Reduction of Area after SSRT of Samples Treated at 600°C/24 h

%Deformation	%Elongation (Normalized)	%RA (Normalized)	Mode of Failure
0	12.19	12.19	Brittle
20	39.91	45.36	Brittle
40	50.2	56.67	Brittle
60	87.62	73.62	Ductile
80	—	—	—

TABLE 4
Percentage Elongation and Reduction of Area after SSRT of Samples Treated at 700°C/24 h

%Deformation	%Elongation (Normalized)	%RA (Normalized)	Mode of Failure
0	28.39	33.48	Brittle
20	93.16	80.96	Ductile
40	78.88	82.36	Ductile
60	—	—	—
80	—	—	—

the grain boundary (and other chromium-depleted regions). The DOS measured by the DL-EPR indicates the total area adjoining the grain boundary (as well as any area within the matrix), which has a chromium concentration less than the critical value. This stems from the fact that any and all such regions remain active, even during repassivation in the DL-EPR. IGSCC, on the other hand, is neither sensitive to the width nor the area of the chromium-depleted region. A grain boundary lacking a critical chromium concentration, irrespective of the width of the chromium-depleted zone, is susceptible to IGSCC. Put in another way, DOS represents two-parameter chromium depletion (depth and width) while IGSCC susceptibility is defined primarily by a single parameter (depth) along with the continuity of a sensitized grain boundary path in the material. This is one of the important reasons for the lack of correspondence between two entities, e.g., DOS and IGSCC observed in undeformed samples sensitized at different conditions. However, this is not the sole determining factor.

When the material is deformed, chromium-depleted regions within the grains develop, in addition to those along the grain boundaries. The DOS does not differentiate between those two regions. The intra-

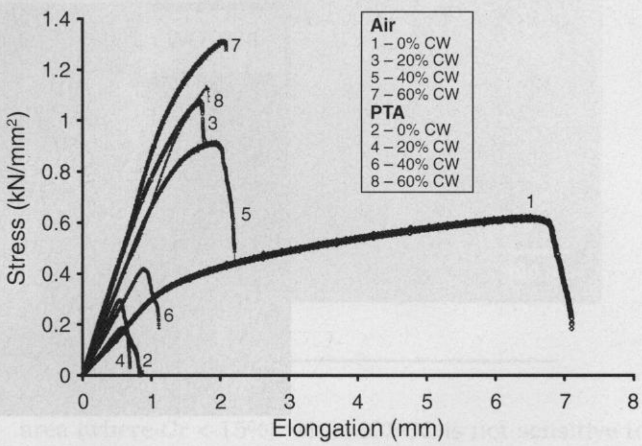

FIGURE 5. *Stress-elongation curves of specimens treated at 600°C/24 h.*

grain regions of chromium depletion are dislocation substructures, slip bands, and other substructural features. The appearance of these features further reduces the correspondence between the DOS and IGSCC susceptibility. The chromium depletion at the grain boundaries is less intense because of the presence of these additional sinks for chromium diffu-

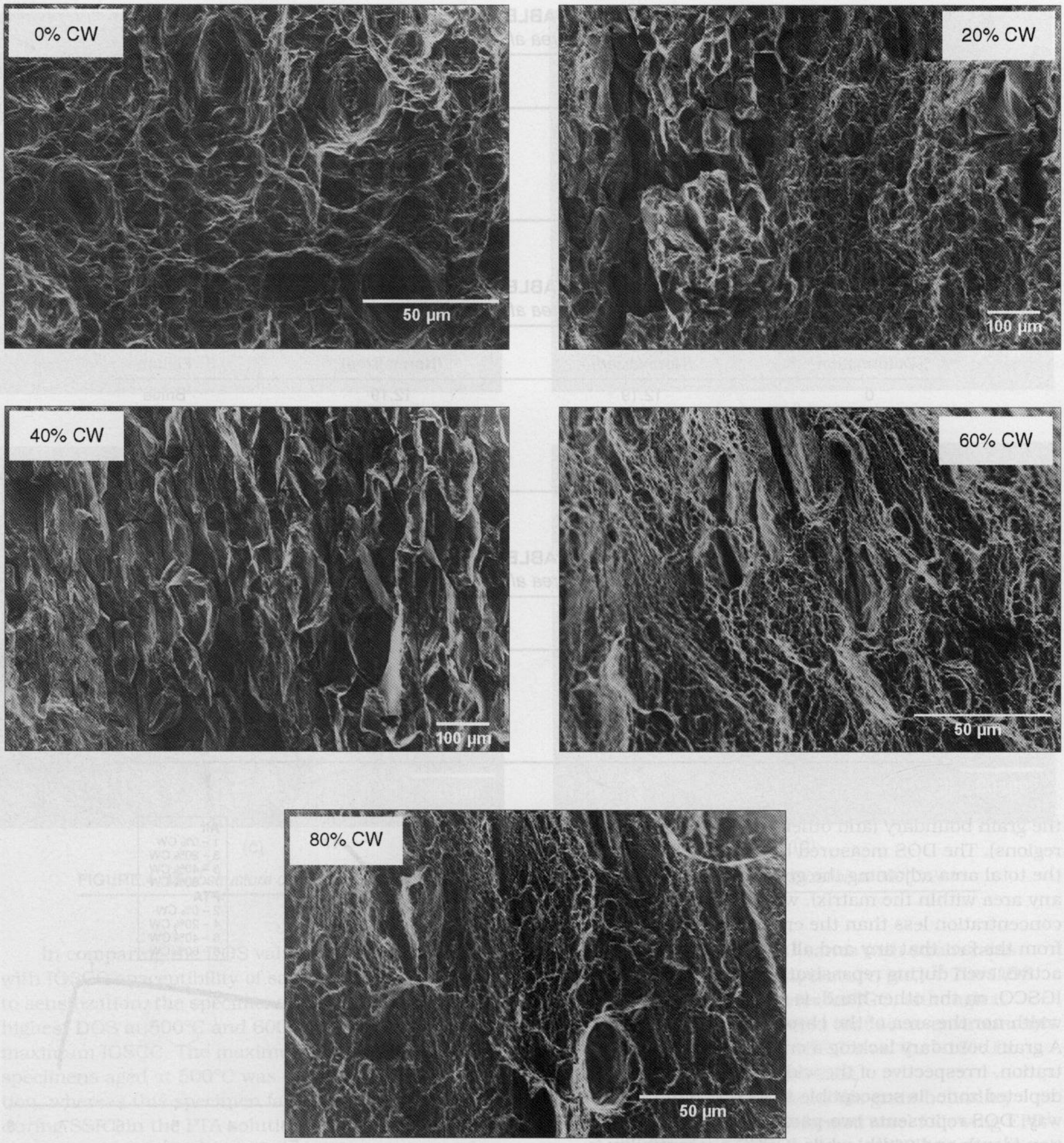

FIGURE 6. *Fractographs of samples treated at 500°C/24 h after fracture during SSRT.*

sion. The loss in correlation between DOS and IGSCC is due to the fact that IGSCC occurs only at grain boundaries. Cracking does not occur at the chromium-depleted intragrain regions for two reasons. First, intragrain regions are not continuous through the material, unlike the grain boundaries that can provide a continuous path for crack propagation. Second, chromium depletion at these substructures may have attained a value detectable by DL-EPR but may not have attained a value low enough to cause SCC. Irrespective of the reason, because IGSCC occurs (by definition) along grain boundaries and the CDZ width is not pertinent to IGSCC susceptibility, the correlation between DOS and IGSCC intensity is not always good.

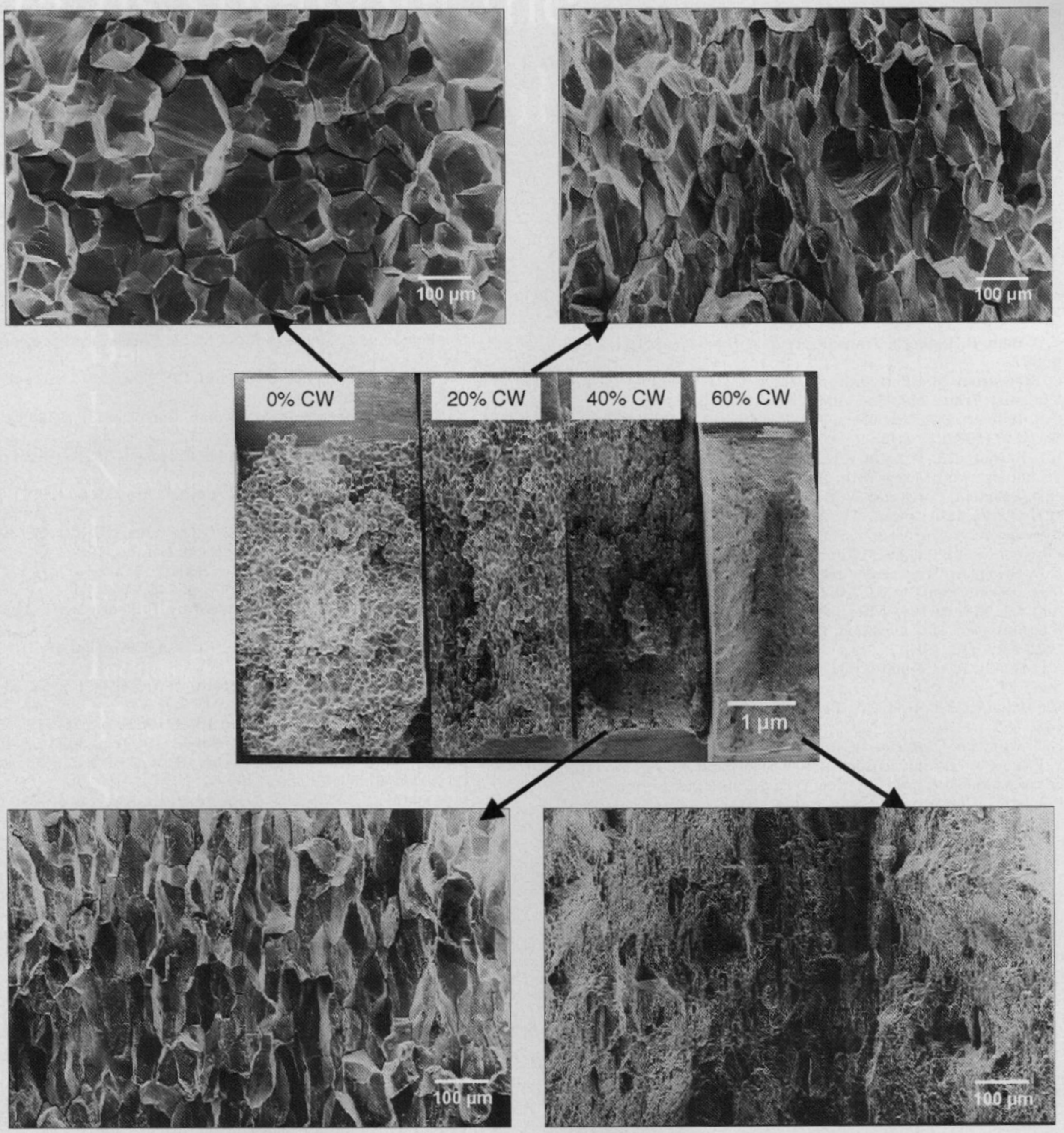

FIGURE 7. *Fractographs of samples treated at 600°C/24 h after fracture during SSRT.*

CONCLUSIONS

❖ The DOS of AISI 304 SS showed maxima with respect to the percentage of deformation. The position of these maxima shift toward lower deformation (from 60% to 20%) with an increase in temperature of sensitization. Deformation, prior to sensitization at 700°C/24 h, was found to desensitize the SS.

❖ The IGSCC susceptibility for the predeformed and undeformed samples did not show a one-to-one correspondence with the DOS value. This is because DOS provides a measure of the total chromium-depleted area (where Cr < 15%), while IGSCC is not sensitive to the width or area but only to the minimum chromium concentration. Additionally, DOS of the sensitized AISI 304 SS after deformation measures the chromium depletion along the grain boundary as well as within the grain interiors such as slip bands and dislocation cells. However, IGSCC susceptibility remains unaffected by these intragrain chromium-depleted regions, since it occurs by definition along the grain boundaries. Samples deformed by 60% or more followed by sensitization at different temperatures did not show any IGSCC irrespective of DOS. Deformation prior to sensitization at 700°C/24 h seems to be useful for IGSCC resistance in the polythionic acid solution.

ACKNOWLEDGMENTS

This work was carried out as an in-house project. The authors acknowledge the Engineering Division for fabricating tensile specimens for this study. The useful discussions with S. Tarafdar on SSRT and fractography are gratefully acknowledged.

REFERENCES

1. E.C. Bain, R.H. Aborn, Trans. Amer. Soc. Steel Treat. 18 (1930): p. 837.
2. C. Stawstrom, M. Hilert, J. Iron Steel Inst. 207 (1969): p. 77-85.
3. K.T. Aust, Trans. Met. Soc. AIME 245 (1969): p. 2,117.
4. C.S. Tedmon, D.A. Vermilyea, J.H. Rosolowski, J. Electrochem. Soc. 118 (1971): p. 192.
5. R.L. Kowan, C.S. Tedmon, Advances in Corrosion Science and Technology, vol. 3 (New York, NY: Plenum Press, 1973), p. 293.
6. H.D. Solomon, Corrosion 34, 6 (1978): p. 183-193.
7. W.L. Clarke, R.L. Cowan, W.L. Walker, ASTM STP 656, "Intergranular Corrosion of Stainless Alloys" (West Conshohocken, PA: ASTM International, 1978), p. 99.
8. H.D. Solomon, "Weld Sensitization," in Proc. Seminar on Counter Measures for Pipe Cracking in BWR's WS-79-174, vol. 2 (Palo Alto, CA: Electric Power Research Institute [EPRI], 1980).
9. P.L. Andresen, H.D. Solomon, D.F. Taylor, EPRI Final Report EPRI-NP-1823, 1981.
10. C.L. Briant, R.A. Mulford, E.L. Hall, Corrosion 38, 9 (1982): p. 468-477.
11. R.A. Mulford, E.L. Hall, C.L. Briant, Corrosion 39 (1983): p. 132-143.
12. H.D. Solomon, Corrosion 40 (1984): p. 51-60,
13. V. Cihal, "Intergranular Corrosion of Steels and Alloys," Material Science Monograph No. 18 (New York, NY: Elsevier Science Publishing Company, 1984), p. 146-49.
14. C.L. Briant, S.K. Banerji, Int. Met. Rev. 23, 4 (1978): p. 164-199.
15. S.M. Bruemmer, Corrosion 42, 1 (1986): p. 27-35.
16. S.M. Bruemmer, L.A. Charlot, Scr. Metall. 20 (1986): p. 1,019-1,024.
17. M.J. Povich, P. Rao, Corrosion 34, 8 (1978): p. 269.
18. H.D. Solomon, Corrosion 41, 9 (1985): p. 512-517.
19. H.E. Hanninen, Int. Met. Rev. 3 (1979): p. 80-135.
20. H.D. Solomon, D.C. Lord, Corrosion 36, 8 (1980): p. 395-399.
21. E.L. Hall, C.L. Briant, Metall. Trans. 15A (1984): p. 793.
22. S.M. Bruemmer, L.A. Charlott, B.W. Arey, Corrosion 44, 6 (1988): p. 328-333.
23. A.P. Majidi, M.A. Streicher, Corrosion 40, 9 (1984): p. 445-458.
24. C.L. Briant, A.M. Ritter, Scr. Metall. 13 (1979): p. 177-181.
25. C.L. Briant, A.M. Ritter, Metall. Trans. 11A, 12 (1980): p. 2,009-2,017.
26. L.E. Murr, A.H. Advani, S. Shankar, D.G. Atteridge, Mater. Character. 24 (1990): p. 135-158.
27. A.H. Advani, D.G. Atteridge, L.E. Murr, S.M. Bruemmer, R. Chelakara, Scr. Metall. Mater. 25 (1991): p. 461-465.
28. A.H. Advani, L.E. Murr, D.G. Atteridge, R. Chelakara, S.M. Bruemmer, Corrosion 47 (1991): p. 939-947.
29. R. Beltran, J.G. Maldonadoo, L.E. Murr, W.W. Fisher, Acta Mater. 45, 10 (1997): p. 4,351-4,360.
30. C. Gracia, F. Martin, P. Tiedra, J. Heredero, M.L. Aaricio, Corrosion 56, 3 (2000): p. 243-255.
31. C. Gracia, F. Martin, P. Tiedra, J. Heredero, M.L. Aaricio, Corros. Sci. 43, 8 (2001): p. 1,519-1,539.
32. R. Singh, P.K. Dey, A. Kumar, S.K. Das, R. Kumar, I. Chattoraj, "Intergranular Corrosion of Deformed SS304," in Proc. National Seminar on Corrosion and its Prevention (NSCP-2001), held December 13-14 (Jamshedpur, India: NML, 2001), p. 21-23.
33. R. Singh, B.R. Kumar, A. Kumar, P.K. Dey, I. Chattoraj, Metall. Trans. 34A, 11 (2003): p. 2,441-2,447.
34. N. Parvathavarthini, R.K. Dayal, J. Nucl. Mater. 305, 2-3 (2002): p. 209-219.
35. R.W. Cochran, R.W. Staehle, Corrosion 24 (1968): p. 369.
36. M. Kowaka, H. Fujikawa, Sumitomo Search 7 (1972): p. 10.
37. H.P. Hawkes, F.H. Beck, M.G. Fontana, Corrosion 19 (1963): p. 247t.
38. P. Muraleedharan, H.S. Khatak, J.B. Gnanamoorthy, P. Rodriguez, Metall. Trans. 16A (1985): p. 285-289.
39. C.H. Samans, Corrosion 24 (1964): p. 256t-262t.
40. S. Ahemad, M.L. Mehta, S.K. Saraf, I.P. Saraswat, Corrosion 37 (1981): p. 412-415.
41. S. Ahemad, M.L. Mehta, S.K. Saraf, I.P. Saraswat, Corrosion 38 (1982): p. 347-353.
42. R. Bandy, R. Roberge, R.C. Newman, Corrosion 39 (1983): p. 391-398.
43. H.S. Isaacs, B. Vyas, M.W. Kendig, Corrosion 38, 3 (1982): p. 130-136.
44. E.A. Ashour, E.A. Meguid, B.G. Ateya, Corrosion 53 (1997): p. 612-616.
45. S.M. Bruemmer, L.A. Charlot, D.G Atteridge, NUREG/CR-3918, U.S. Nuclear Regulatory Commission, October 1984.
46. F.P. Ford, M.J. Povich, Corrosion 35 (1979): p. 569.
47. E. Truman, Corros. Sci. 17 (1977): p. 746.
48. P. Muraleedharan, J.B. Gnanamoorthy, P. Rodriguez, Corrosion 52 (1996): p. 790-800.
49. S.M. Bruemmer, B.W. Arey, L.A. Charlot, Corrosion 48, 1 (1992): p. 42-49.
50. G.S. Was, V.B. Rajan, Metall. Trans. 18A, 7 (1987): p. 1,313-1,323.
51. G.S. Was, V.B. Rajan, Corrosion 43, 9 (1987): p. 576-579.
52. S.M. Bruemmer, Mater. Sci. Forum 46 (1989): p. 309.
53. D.B. Wells, J. Stewart, A.W. Herbert, P.M. Scot, P.E. Williams, Corrosion 45, 8 (1989): p. 649-660.
54. M.A. Gaudett, J.R. Scully, J. Electrochem. Soc. 140 (1993): p. 3,425-3,437.
55. M.K. Ahn, H.S. Kwon, J.H. Lee, Corrosion 51 (1995): p. 441.
56. R.M. Kruger, S.F. Claeys, G.S. Was, Corrosion 41, 9 (1985): 504-512.
57. H. Hanninen, "Intergranular Stress Corrosion Cracking," Final Report of the NKA Project MAT 530, VTT, Finland, 1989.
58. ASTM Standard Designation A262-Practice A-F, "Standard Practices for Detecting Susceptibility to Intergranular Attack in Austenitic Stainless Steels," vol. 03.02 (West Conshohocken, PA: ASTM International, 1993), p. 1-16.
59. S. Pednekar, S. Smailowska, Corrosion 36, 10 (1980): p. 565-577.
60. C.S. Barret, T.B. Massalski, in Structure of Metals (New Delhi, India: Eurasia Publishing House, 1968), p. 91.
61. ASTM Standard Designation G35-88, "Standard Practice for Determining the Susceptibility of Stainless Steels and Related Nickel-Chromium-Iron Alloys to Stress-Corrosion Cracking in Polythionic Acids," vol. 03.02 (West Conshohocken, PA: ASTM International, 1998), p. 127-29.
62. K. Eleyaperumal, P.K. De, J. Balachandra, Corrosion 28 (1972): p. 269-73.
63. V. Seetharaman, K. Krishnan, J. Mater. Sci. 16 (1981): p. 523-30.
64. G.E. Dieter, in Mechanical Metallurgy (U.K.: McGraw-Hill Book Co., Ltd., 1988), p. 232.